Anomalous persistent photoconductivity in Cu_2ZnSnS_4 thin films and solar cells

A. Abelenda[1, 2], M. Sánchez[2], G. M. Ribeiro[1], P. A. Fernandes[3,5], P. M. P. Salomé[4], A. F. da Cunha[5], J. P. Leitão[5], M. I. N. da Silva[6] and J. C. González[1, *]

[1]Departamento de Física, Universidade Federal de Minas Gerais, 30123-970 Belo Horizonte, Minas Gerais, Brasil.
[2]Facultad de Física, Universidad de La Habana, Colina Universitaria, C.P. 10400 Habana, Cuba.
[3]Departamento de Física, Instituto Superior de Engenharia do Porto, Instituto Politécnico do Porto, Rua Dr. António Bernardino de Almeida, 431, 4200-072 Porto, Portugal.
[4]International Iberian Nanotechnology Laboratory, LaNaSC - Laboratory for Nanostructured Solar cells, Av. Mestre José Veiga, 4715-330 Braga, Portugal.
[5]Departamento de Física e I3N, Universidade de Aveiro, Campus Universitário de Santiago, 3810-193 Aveiro, Portugal.
[6]Centro Universitário UNA, Campus Universitário Linha Verde, 31744-007 Belo Horizonte, Minas Gerais, Brasil.

*Corresponding author: gonzalez@fisica.ufmg.br

Persistent photoconductivity effect (PPC) has been investigated in Cu_2ZnSnS_4 thin films and solar cells as a function of temperature. An anomalous increase of the PPC decay time with temperature was observed in all samples. The PPC decay time activation energy was found to increase when temperature rises above a crossover value, and also to growth with the increase of the sulphurization temperature and pressure. Both, the anomalous behavior of the PPC decay time and the existence of two different activation energies are explained in terms of local potential fluctuations in the band edges of CZTS.

1 Introduction

More than 20 companies in the world produce $CuIn_xGa_{1-x}Se$ (CIGS) based solar cells modules at commercial scale or in earlier stages of production [1, 2]. CIGS exhibits the highest thin film solar cell efficiency [3]. However, due to the increasing price and scarcity high cost of Indium and Gallium, $Cu_2ZnSn(S,Se)_4$ (CZTSSe) has been proposed to replace the CIGS absorber layer in order to obtain Indium free thin film solar cells [4]. In the past few years several groups have fabricated CZTSSe-based solar cells and reach power conversion efficiencies of 12.6 % and 9.2 % for CZTSSe [5] and pure sulphur (CZTS) [6] solar cells, respectively. These values are still well below of the predicted theoretical limit of approximately 30 %, indicating the necessity of further studies of the photoelectrical properties of these materials. In fact, the photoelectrical instabilities and metastabilities of $CuInGaSe_2$ (CIGS) have been well studied [7 - 9]. However, the available information about the CZTS photoelectrical properties are still very limited [10 - 14].

Persistent photoconductivity (PPC) is a light-induced enhancement in the conductivity that persists for a long period of time after the termination of light excitation. This phenomenon

has been observed in several semiconductors [15 - 18]. PPC provides information on carrier storage and relaxation mechanism in semiconductors materials. Although PPC can be advantageously utilized in photonic devices such as optical switches and others [19 - 21], it causes undesirable effects in solar cells and other devices [22 - 24]. Therefore, it is important to understand the origin of PPC for both, fundamental reasons and due to the influence in devices.

PPC in semiconductors materials is often explained by two different models. The large lattice relaxation model (LLR) is based on a strong interaction between the electrons in a defect state and the local lattice configuration in the neighborhood of the defect, such as for *DX* and *EL2* centers [25, 26]. The small capture cross section of the traps prevents, at low temperatures, the capture of photoexcited electrons from the conduction band and leads to the observation of PPC. In contrast, the barrier model relates PPC with local changes of the electrical potential, where the photogenerated electron-hole pairs are spatially separated [17, 27 - 29]. In this case, it is necessary to distinguish between intentionally fabricated macroscopic barriers (e.g.: quantum wells, superlattices) [27, 28], and unintended band bending [17] or random potential fluctuations that can occur in the semiconductor structure [29].

In this work we report an anomalous PPC effect in several CZTS thin films and a solar cell. Anomalous PPC was observed in samples prepared under different sulphurization conditions of pressure, time and temperature. The measurements were performed on a temperature range between 4.8 K to 300 K and two different activation energies were obtained for the temperature dependence of the PPC decay time. Both, the anomalous behavior of the PPC and the existence of two different activation energies are explained in terms of local potential fluctuations in the band edges of CZTS.

2 Experimental details

Cu_2ZnSnS_4 thin films were prepared by sequential deposition of precursor thin layers of Zn, Sn and Cu on a soda-lime glass (SLG) substrate followed by a sulphurization step as reported elsewhere [10, 30, 31]. The precursors were deposited by DC magnetron sputtering and the sulphurization was done by thermal annealing in sulphur vapour atmosphere. Two sets of samples were studied, one was annealed at P = 5 Torr and different temperatures, while a second set was prepared at different sulphur pressures and approximately the same sulphurization temperature. A complete CZTS-based solar cell with the standard SLG/Mo/CZTS/CdS/i-ZnO/ZnO:Al/Ni-Al grids structure was also studied. The growth conditions of the thin films as well as the CZTS absorber layer of the solar cell are summarized in Table I.

Table 1 Growth conditions and PPC parameters for the samples of this study. P, T_S and t_S are the sulphurization pressure, temperature and time, respectively. E_L and E_H are the characteristic decay time activation energies for the low and high temperature regions, respectively. T_c is the crossover temperature between both regions.

Sample	Growth conditions			E_A (meV)		T_c (K)
	P (Torr)	T_S (ºC)	t_S (min.)	E_L	E_H	
S08	5	563	30	2.9	14.5	80

S11	5	476	30	3.2	8.3	40
S19	5	424	30	1.2	7.5	40
S28	20	515	10	0.4	6.6	30
S29	50	517	10	0.4	14.0	40
Cell	0.5	525	10	0.6	7.8	20

The surface morphology of the samples was studied by Scanning Electron Microscopy (SEM) and Atomic Force Microscopy (AFM), while the structural properties were investigated by X-ray diffraction (XRD) and Raman spectroscopy (RS).

For the PPC measurements of the CZTS thin films Au contacts were placed at the edges of 25 mm^2 samples and the current passing through two diagonal contacts was measured as a function of time with a DC applied bias voltage of 100 mV. In the solar cell case, the front and back contacts were used to measure the PPC. The measurements were carried out in the temperature range from 4.8 K to 300 K. A 1.32 eV light emitting diode (LED) with power densities between 14 and 56 $\mu W/cm^2$ was used as a light source to excite the samples.

3 Results and discussion

Figure 1 shows the typical surface's morphology of the thin films as obtained by AFM and SEM. Large grains of about 500 nm were observed next to smaller grains of about 100 nm. The large surface roughness in some areas is possibly due to the removal of unwanted $Cu_{2-x}S$ phases by KCN etching [25]. Figure 1(c) shows a typical X-ray diffraction (XRD) pattern of the films, with a preferential (112) orientation. The average crystallite size of the samples was estimated in 146 nm from the full width at half maximum of the XRD patterns peaks and by using the Scherrer's formula [32]. A typical Raman spectrum of the films is also shown in figure 1(d), where Lorentzian functions were used to deconvolute the spectrum into individual Raman peaks. The Raman spectrum is dominated by CZTS peaks, as well as the XRD pattern, although residual amounts of ZnS were also detected [33].

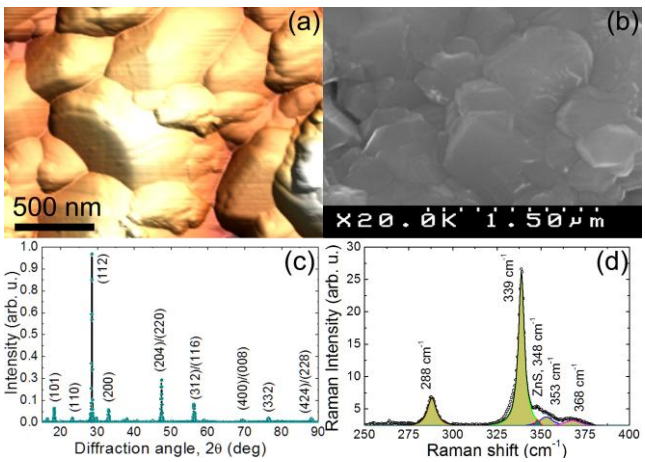

Figure 1 AFM (a) and SEM (b) images of the surface of sample S28. The Z scale of image (a) is 330 nm. (c) XRD diffractogram and (d) Raman spectrum the sample .

Figure 2(a) shows the general behavior of the photoconductivity of sample S28 at 300 K for three different illumination power densities. A rapid increase of the photocurrent can be observed when the illumination from the LED is turned on, reaching a saturation after approximately 40 seconds. When the illumination is turned off the photocurrent decays almost exponentially showing a persistency for more than 100 seconds. An increase in the illumination intensity increases the saturation photocurrent, but does not alter significantly the shape of the decay curves and the decay time constant.

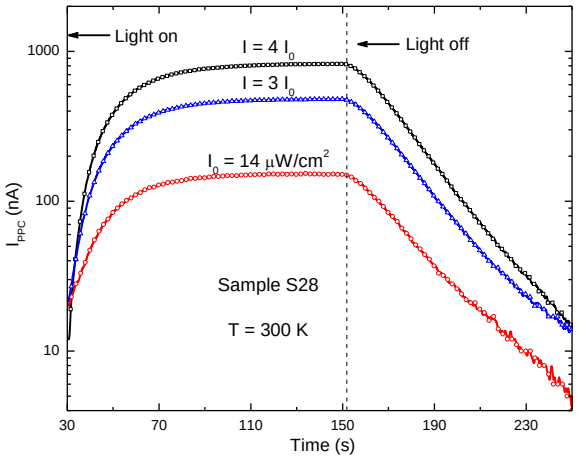

Figure 2 Photocurrent curves of sample S28 at 300 K under different illumination intensities.

Figure 3 shows three PPC decay curves measured for sample S19 at different temperatures. For comparison purposes the PPC current $I_{PPC}(t) = I(t) - I_{dark}$ was normalized to unity at time $t = 0$ *s*, when the illumination was turned off. I_{dark} is the dark current, i.e the current level before the illumination was turned on. It should be note that the PPC effect is present in the entire measured temperature range for tens of seconds and it is enhanced as the temperature increases. This is an unexpected result since the opposite behavior has been widely reported by several authors in different materials [16, 18, 34 - 36]. The PPC decay curves have been fitted by other authors using different functions [27, 36 - 38]. However, in this case, the PPC decays curves show a stretched-exponential behavior described for the whole temperature range with the Kohlrausch expression [39],

$$I_{\mathrm{PPC}}(t) = I_0 \exp\left[-\left(\frac{t}{\tau}\right)^{\beta}\right], \qquad (1)$$

where τ and β are two decay characteristic parameters for each measured temperature. τ is the characteristic decay time or relaxation time constant and β ($0 < \beta < 1$) is the decay exponent. It is worth nothing that $I_0 = I_{\mathrm{PPC}}(0) = 1$, according the chosen normalization. Fitting of the experimental data of the PPC decay curves with eq. (1) allows the extraction of both, τ and β parameters.

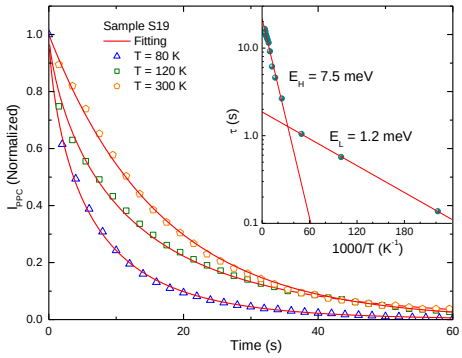

Figure 3 PPC decay curves for three different temperatures measured in sample S19. The solid lines correspond to the fitting of the experimental data with eq. (1). Inset: Arrhenius plot of the extracted relaxation time constant as a function of temperature.

The inset of Figure 3 shows an Arrhenius plot [$\tau = \tau_0 \exp(-E_A/kT)$] of the PPC characteristic decay time of sample S19. The unexpected (anomalous) increase of the characteristic decay time with temperature is evident. Two temperature regions denoted by different values of the activation energy (E_A) can be also observed, with lower activation energy (E_L) value in the low temperature region and higher activation energy (E_H) value in the high temperature region. The same behavior was observed in all samples, including the solar cell. The activation energies (E_L and E_H) for the low and high temperature ranges, as well as the crossover temperature (T_c) between the two regions are summarized in Table 1. A slight increase of the values of the activation energies E_L and E_H as well as the crossover temperature T_c can be observed as the sulphurization temperature and pressure increases.

Figure 4 shows scaled PPC decay curves for the CZTS-based solar cell measured at 100 K after photoexcitation with four different LED power outputs. The scaled time is the ratio t/τ, being τ the characteristic decay time constant obtained for each LED output power. Inset of Figure 4 shows the decay exponent β versus temperature at a fixed LED light intensity. Clearly β shows a propensity to increase with temperature. This behavior was observed in all samples.

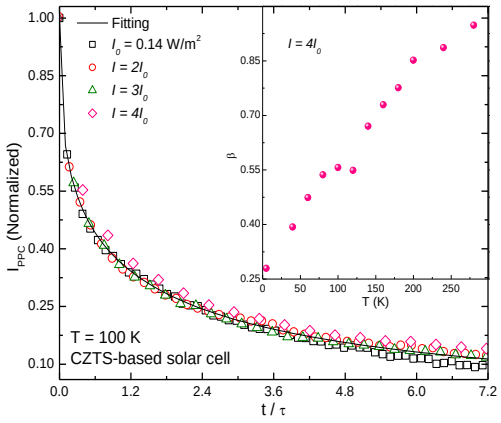

Figure 4 Scaled PPC decay curves obtained for the CZTS-based solar cell at 100 K for four different LED light intensities. The fit of the experimental data with eq. (1) is represented by the solid line. Inset: the decay exponent β versus temperature plot, for a fixed LED light intensity.

As we can see in figure 4 all curves have the same stretching, demonstrating the independence between the decay parameter β and the LED output power. The curves were fitted by a single stretched-exponential function with the same value of the decay exponent, β = 0.39. This behavior of PPC decay curves indicates that the origin of the PPC is the same over the entire temperature range studied here.

The anomalous behavior observed for the PPC effect in CZTS can be qualitatively explained in terms of local potential fluctuations in the energy band edges. Electrostatic local potential fluctuations will spatially separate the photo-excited free carriers reducing their probability of recombination giving rise to a PPC effect. These fluctuations could be caused by elevated doping levels and high degree of compensation in the films [10, 40, 41]. In highly compensated materials, such as the CZTS thin films [42, 43], most defects are ionized and the free carrier concentration is low. Therefore, the random distribution of charged and unscreened defects causes local electrostatic potential fluctuations, which in turn shifts the conduction and valence band edges below and above their positions in a pure uncompensated semiconductor, respectively. A simplified band diagram illustrating these fluctuations is shown in figure 5. In the figure, E_g^0, E_c^0, and E_v^0 correspond to the band gap energy and the edges of the conduction band and valence band, respectively, in the flat band approximation. Due to the local potential fluctuations the band gap energy could be reduced to Eg^{eff} *and* E_c and E_v are the percolation levels of electrons and holes, respectively. Above E_c and E_v electrons and holes, respectively, can be considered free carriers. The conduction $\rho_c(E)$ and valence $\rho_v(E)$ band density of states, as well as the density of states related to the acceptors $\rho_a(E)$ are also represented in figure 5. Deeps of potential wells are random, and while for wells with typical potential depths it is assumed that there are no bound states, this is not the case for deeper wells, which exist in smaller proportion. These deeper wells appear where large clusters of donors or acceptors bend the bands strongly. On the other hand, the potential wells of the conduction band are deeper than those of the valence band because of the small electron effective mass. At low temperatures, photo-excited carriers are distributed in localized tail states in quasiequilibrium. Since the holes (electrons) cannot approach the donor (acceptors) wells too closely, electrons (holes) can only recombine with holes (electrons) localized on distant acceptors (donors), a process with a relatively low probability of occurrence. This process is called tail-impurity (TI) recombination. There are two separate TI recombination channels: a channel related to deeper wells referred to as TI-A [41] and a channel related to shallower wells referred to as TI-B [41].

We have previously shown that the low temperature optical emission from CZTS thin films present a broad and asymmetric band centered at 1.24 eV [42, 44]. As temperature increases, the band shifts linearly to lower energies. The energy position of the band is also very sensitive to the excitation power, shifting to higher energies as the excitation power increases. The origin of this band can be ascribed mainly to the recombination of electrons localized in tails of the conduction band with holes bound to acceptor impurities (TI transitions), broadened by the presence of local potential fluctuations [40 - 42, 44].

In the photocurrent experiments, at low temperatures, photo-excited carriers remain localized at the local minima and maxima of the conduction and valence bands, respectively. In order to recombine holes are first non-radiatively transferred to the acceptors band, before to

recombine radiatively with electrons in tails of the conduction band. Since electrons (holes) cannot approach the acceptors (donors) wells too closely, the localization decreases the recombination probability allowing the PPC effect to take place. However, as temperature slightly increases, the electrons and holes localized in shallow potential wells can drift to deeper wells being more separated and slightly increasing the PPC characteristic decay time with a small thermal activation energy E_L. At higher temperatures, above the crossover temperature T_c, the local potential fluctuations are reduced and the bands flattened and electrons and holes can only be localized at deep potential wells created by large charge clusters. Under these conditions, the electron and holes pairs are further spatially separated increasing the characteristic decay time with a large thermal activation energy (E_H). This model does not only explains the observed temperature behavior of the PPC characteristic decay time in our experiments, but it is also in agreement with the previously reported photoluminescence studies carried out in similar CZTS thin films [42].

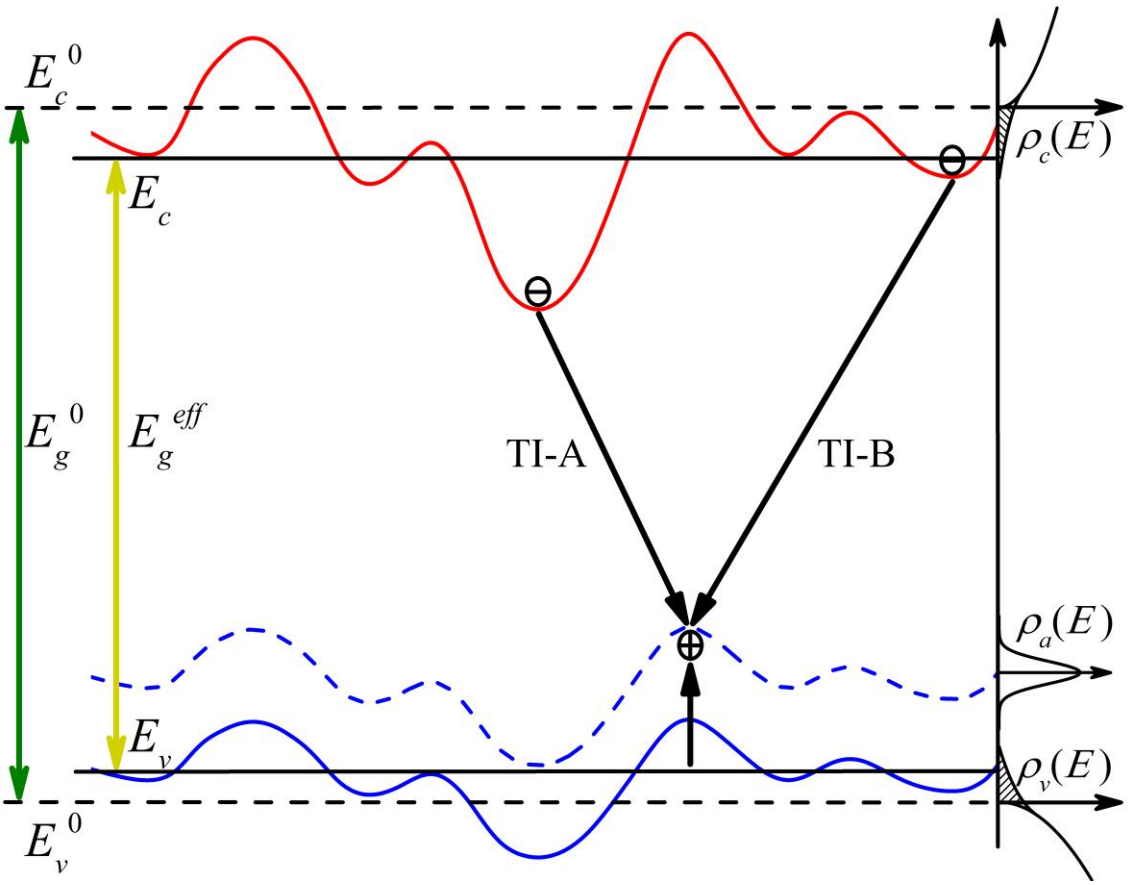

Figure 5 Simplified band diagram of a CZTS thin film showing the fluctuations of the band edges and acceptors band, as well as the TI optical transition.

The origin of the local potential fluctuations in CZTS is still unknown. Here electrostatic fluctuations created by charged and unscreened defects were considered. In this case the band edges will remain essentially parallel to each other, but the amplitude of the potential fluctuations in the valence band will be reduced due to the large value of the holes effective mass. This mechanism is only significant in highly doped and strongly compensated materials, as the CZTS thin films, because there are no enough carriers to shield the clusters of charged

defects. Nano-scale clusters of Zn_{Cu} anti-site donors have already been reported in CZTS [45]. However, local potential fluctuations are also reported to be caused by compositional fluctuations in sulphur and selenium-based II-VI semiconductor alloys [16, 34-36]. In this case, fluctuations in the conduction and valences band edges will be opposite, leaving them antiparallel to each other. The observed fact that the decay time activation energies changes with the sulphurization conditions could indicates a correlation with the improvement of the stoichiometry and composition uniformity of the samples. However, the doping level and degree of compensation are also changed by the sulphurization conditions in CZTS [43].

4 Conclusions

In summary, photoelectrical properties of several CZTS thin film samples and a CZTS-based solar cell were studied. In particular the persistent photoconductivity effect was observed in these samples and studied as function of temperature. An anomalous behavior of the temperature dependence of the PPC decay time constant was obtained for all samples including the solar cell. The decay constant increases as a function of temperature with an Arrhenius behavior, but with two different activation energies at the low and high temperature regions. The values of the activation energies as well as the crossover temperature between the low and high temperature regions were found to slightly increase with the sulphurization temperature and pressure. The anomalous behavior was attributed to the presence of electrostatic local potential fluctuations in the electronic band structure of the samples. Our results suggest that the electrostatic fluctuations dominate the PPC effect in CZTS thin film, but do not exclude the presence of compositional fluctuations in the samples. With regards to the solar cells, the exact measurement conditions that would allow extracting more information about the generation, transport and recombination mechanism inside and outside of the p-n junction are still to be explored. Therefore, further investigations are needed to better understand the PPC effect in CZTS thin film and solar cells.

Acknowledgements We would like to acknowledge the financial support of the Brazilian agencies CAPES, CNPq and FAPEMIG. The authors acknowledge the financial support from the Portuguese Science and Technology Foundation (FCT), through the grants PTDC/CTM-MET/113486/2009, PEST-C/CTM/LA0025/2011 and RECI/FIS-NAN/0183/2012. P. M. P. Salomé acknowledges the financial support of the European Commission via FP7 Marie Curie IEF 2012 Action No. 327367.

References

[1] A. Jager-Waldau, Progress in chalcopyrite compound semiconductor for photovoltaic applications and transfer of results into actual solar cell production, Sol. Energy Mater. & Sol. Cells 95 (2011) 1509-1517.

[2] P. Reinhard, S. Buecheler, A. N. Tiwari, Technological status of Cu(In,Ga)$(Se,S)_2$-based photovoltaics, Sol. Energy Mater. & Sol. Cells 119 (2013) 287-290.

[3] P. Jackson, D. Hariskos, R. Wuerz, W. Wischmann, and M. Powalla, Compositional investigation of potassium doped Cu(In,Ga)Se_2 solar cells with efficiencies up to 20.8%, Phys. Status Solidi (RRL) 8 (2014) 219-222.

[4] A. Polizzotti, I. L. Repins, R. Noufi, S-H. Wei, D. B. Mitzi, The state and future prospects of kesterite photovoltaics, Energy Environ. Sci. 6 (2013) 3171-3182.

[5] Kato, H. Hiroi, N. Sakai, S. Muraoka, H. Sugimoto, Characterization of front and back interfaces on Cu_2ZnSnZ_4 thin-film solar cells, 27th Eur. Photovolt. Sol. Energy Conf. and Exhib. (2012) 2236-2239.

[6] B. Shin, O. Gunawan, Y. Zhu, N. A. Bojarczuk, S. J. Chey, S. Guha, Thin film solar cell with 8.4% power conversion efficiency using an earth abundant Cu_2ZnSnS_4 absorber, Prog. Photovolt.: Res. and Appl. 21 (2013) 72-76.

[7] U. Rau, M. Schmitt, J. Parisi, W. Riedl F. Karg, Persistent photoconductivity in $Cu(In,Ga)Se_2$ heterojunctions and thin films prepared by sequential deposition, Appl. Phys. Lett. 73 (1998) 223-225.

[8] M. Igalson, P. Zabierowski, Transient capacitance spectroscopy of defect levels in CIGS devices, Thin Solid Films 361 (2000) 371-377.

[9] J. H. Schön, E. Bucher, Persistent photoconductivity in n- and p-type $CuGaSe_2$, J. Phys. D: Appl. Phys. 34 (2001) 25-29.

[10] J. C. González, G. M. Ribeiro, E. R. Viana, P. A. Fernandes, P. M. P. Salomé, K. Gutiérrez, A. Abelenda, F. M. Matinaga, J. P. Leitão, A. F. da Cunha, Hopping conduction and persistent photoconductivity in Cu_2ZnSnS_4 thin films, J. Phys. D: Appl. Phys. 46 (2013) 155107(7pp).

[11] J. Feng, S. Honglie, W. Wei, Optical and electrical properties of Cu_2ZnSnS_4 film prepared by sulfurization, J. Electron. Mat. 41 (2012) 2204-2209.

[12] F. Jiang, H. Shen, Research on the photoresponse current and photosensitive properties of Cu_2ZnSnS_4 thin film prepared by sulfurization of a sputtered metal precursor, RSC Adv. 3 (2013) 23474-23481.

[13] K. R. Choudhury, Y. Cao, J. V. Caspar, W. E. Farneth, Q. Guo, A. S. Ionkin, L. K. Johnson, M. Lu, I. Malajovich, D. Radu, H. D. Rosenfeld, W. Wu, Characterization and understanding of performance losses in a highly efficient solution-processed CZTSSe thin-film solar cell, 38th IEEE Photovolt. Specialists Conf. (2012) 001471-001474.

[14] F. Jiang, H. Shen, J. Jin, W. Wang, Preparation and optoelectronic properties of Cu_2ZnSnS_4 film semiconductor devices, materials, and processing, J. Electrochem. Soc. 159 (2012) H565-H569

[15] R. H. Bube, Mechanism of photoconductivity in microcrystalline powders, J. Appl. Phys. 31 (1960) 2239-2254.

[16] H. X. Jiang, J. Y. Lin, Percolation transition of persistent photoconductivity in II-VI mixed crystals, Phys. Rev. Lett. 64 (1990) 2547-2550.

[17] E. R. Viana, J. C. González, G. M. Ribeiro, A. G. de Oliveira, Photoluminescence and high-temperature persistent photoconductivity experiments in SnO_2 nanobelts, J. Phys Chem. C 117 (2013) 7844-7849.

[18] C. H. Chen, D. R. Hang, W. H. Chen, Y. F. Chen, H. X. Jiang, J. Y. Lin, Persistent photoconductivity in $In_xAl_yGa_{1-x-y}N$ quaternary alloys, Appl. Phys. Lett. 82 (2003) 1884-1886.

[19] T. Thio, R. A. Linke, G. E. Devlin, J. W. Bennett, J. D. Chadi, Writing erasable metallic patterns in insulating $Al_xGa_{1-x}As$:DX, Appl. Phys. Lett. 65 (1994) 1802-1804.

[20] T. Tanabe, M. Notomi, S. Mitsugi, A. Shinya, E. Kuramochi, Fast bistable all-optical switch and memory on a silicon photonic cristal on-chip, Opt. Lett. 30 (2005) 2575-2577.

[21] R. A. Linke, I. Redmond, T. Thio, D. J Chadi, Holographic storage media based on optically active bistable defects, J. Appl. Phys. 83 (1998) 661-673.

[22] T. Meyer, F. Engelhardt, J. Parisi, U. Rau, Spectral dependence and hall effect of persistent photoconductivity in polycrystalline Cu(In,Ga)Se_2 thin films, J. Appl. Phys. 91 (2002) 5093-5099.

[23] M. S. Birrittella, C. Seelbach, H. Goronkin, The effect of backgating on the design and performance of GaAs digital integrated circuits, IEEE Trans. Electron. Devices 29 (1982) 1135-1142.

[24] M. I. Nathan, Photoconductivity in selectively n- and p-doped $Al_xGa_{1-x}As$/GaAs heterostructures, Solid State Electron. 29 (1986) 167-172.

[25] D. V. Lang, R. A. Logan, Large-lattice-relaxation model for persistent photoconductivity in compound semiconductors, Phys. Rev. Lett. 39 (1977) 635-639.

[26] R. M. Rubinger, J. C. Bezerra, E. F. Chagas, J. C. González, W. N. Rodrigues, G. M. Medeiros, M. V. B. Moreira, A. G. de Oliveira, Thermally stimulated current spectroscopy on silicon planar-doped GaAs samples, J. Appl. Phys. 84 (1998) 3764-3769.

[27] H. J. Queisser, D. E. Theodorou, Decay kinetics of persistent photoconductivity in semiconductors, Phys. Rev. B 33 (1986) 4027-4033.

[28] H. J. Queisser, Nonexponential relaxation of conductance near semiconductor interfaces, Phys. Rev. Lett. 54, (1985) 234-236.

[29] M. K. Sheinkman, A. Ya. Shik, Long-term and residual conductivity of semiconductors (review), Fiz. Tekh. Poluprovodn. 10 (1976) 209-233 [Sov. Phys. Semicond, 10 (1976) 128-143].

[30] P. M. P. Salomé, J. Malaquias, P. A. Fernandes, M. S. Ferreira, A. F. da Cunha, J. P. Leitao, J. C. González, F. M. Matinaga, Growth and characterization of $Cu_2ZnSn(S,Se)_4$ thin films for solar cells, Sol. Energy Mater. & Sol. Cells 101 (2012) 147-153.

[31] P. A. Fernandes, A. F. Sartori, P. M. P. Salomé, J. Malaquias, A. F. da Cunha, M. P. F. Graça, J. C. González, Admittance spectroscopy of Cu_2ZnSnS_4 based thin film solar cells, Appl. Phys. Lett. 100 (2012) 233504(4pp).

[32] C. E. Kril, R. Birringer, Estimating grain-size distributions in nanocrystalline materials from X-ray diffraction profile analysis, Phil. Mag. A 77 (1998) 621-640.

[33] P. A. Fernandes, P. M. P. Salomé, A. F. Sartori, J. Malaquias, A. F. da Cunha, Björn-Arvid Schubert, J. C. González, G. M. Ribeiro, Effects of sulphurization on Cu_2ZnSnS_4 absorbers and thin films solar cells from metallic precursors, Sol. Energy Mater. & Sol. Cells 115 (2013) 157-165.

[34] H. X. Jiang, J. Y. Lin, Persistent photoconductivity and related critical phenomenon in $Zn_{0.3}Cd_{0.7}Se$, Phys. Rev. B 40 (1989) 10025-10028.

[35] J. Z. Li, J. Y. Lin, H. X. Jiang, J. F. Geisz, S. R. Kurtz, Persistent photoconductivity in $Ga_{1-x-}In_xN_yAs_{1-y}$, Appl. Phys. Lett. 75 (1999) 1899-1901.

[36] C. Johnson, J. Y. Lin, H. X. Jiang, M. A. Khan, C. J. Sun, Metastabillity and persistent photoconductivity in Mg-doped p-type GaN, Appl. Phys. Lett. 68 (1996) 1808-1810.

[37] G. S. Paul, P. Agarwal, Persistent photocurrent and decay studies in CdS nanorods thin films, J. Appl. Phys. 106 (2009) 103705(5pp).

[38] N. Sarkar, S. Dhar, S. Ghosh, The role of the grain boundary on persistent photoconductivity in GaN, J. Phys.: Condens. Matter 15 (2003) 7325-7335.

[39] R. Palmer, D. L. Stein, E. Abrahams, P. W. Anderson, Models of hierarchically constrained dynamics for glassy relaxation, Phys. Rev. Lett. 53 (1984) 958-961.

[40] V. V. Osipov, T. I. Soboleva, M. G. Foigel, Interpurity radiative recombination in heavily doped semiconductors, Fiz. Tekh. Poluprovodn. 11 (1977) 1277-1288 [Sov. Phys. Semicond. 11 (1977) 752-759].

[41] S. A. Schumacher, J. R. Botha, V. Alberts, Photoluminescence study of potential fluctuations in thin layers of $Cu(In_{0.75}Ga_{0.25})(S_ySe_{1-y})_2$, J. App. Phys. 99 (2006) 063508 (8pp).

[42] J. P. Leitão, N. M. Santos, P. A. Fernandes, P. M. P. Salomé, A. F. da Cunha, J. C. González, G. M. Ribeiro, F. M. Matinaga, Photoluminescence and electrical study of fluctuating potentials in Cu_2ZnSnS_4-based thin films, Phys. Rev. B 84 (2011) 024120(8pp).

[43] J. C. González, P. A. Fernandes, G. M. Ribeiro, A. Abelenda, E. R. Viana, P. M. P. Salomé, A. F. da Cunha, Influence of the sulphurization time on the morphological, chemical, structural and electrical properties of Cu_2ZnSnS_4 polycrystalline thin films, Sol. Energy Mater. & Sol. Cells 123 (2014) 58-64.

[44] J. P. Leitão, N. M. Santos, P. A. Fernandes, P. M. P. Salomé, A. F. da Cunha, J. C. González, F. M. Matinaga, Study of optical and structural properties of $Cu_2ZnSnSe_4$ thin films, Thin Solid Films 519 (2011) 7390-7393.

[45] B. G. Mendis, M. D. Shannon, M. C. J. Goodman, J. D. Major, A. A. Taylor, D. P. Halliday, K. Durose, The nature of electrostatic potential fluctuations in Cu_2ZnSnS_4 and their role on photovoltaic device performance, J. Phys.: Conf. Series 471 (2013) 012014(4pp).